










Impact of loading, heart rate, and short episodes of ischaemia on myocardial stiffness assessed using shear wave elastography in an open-chest animal model

Eric Saloux ^{1,2,*}, Christophe Simard ², Pauline Ruello ³, Adrien Lemaitre¹, Amir Hodzic ¹, Alexandre Lebrun², Pierre-Antoine Dupont², Christophe Tribouilloy ⁴, H el ene Eltchaninoff ⁵, Morgane Le Garc e ⁶, Christophe Fraschini ⁶, Vladimir Saplacan³, and Alain Manrique ^{1,7}; on behalf of the STOP-AS investigators

¹Centre Hospitalier Universitaire de Caen Normandie, Cardiology Department, Avenue de la C ote de Nacre, Caen cedex 14033, France

²UR 4650 PSIR, Universit e de Caen Normandie, GIP Cyceron, Campus Jules Horowitz, BP 5229, 14074 Caen cedex 6, France

³Centre Hospitalier Universitaire de Caen Normandie, Heart Surgery Department, Avenue de la C ote de Nacre, Caen cedex 14033, France

⁴Centre Hospitalier Universitaire Amiens Picardie, Cardiology Department, 1 Rue du Professeur Christian Cabrol, 80000 Amiens, France

⁵Centre Hospitalier Universitaire de Rouen Normandie, Cardiology Department, 37 Bd Gambetta, 76000 Rouen, France

⁶SuperSonic Imagine.SA, Aix-en-Provence, 153 Rue Emilien Gautier, 13290 Aix-en-Provence, France

⁷Centre Hospitalier Universitaire de Caen Normandie, Nuclear Medicine Department, Avenue de la C ote de Nacre, Caen cedex 14033, France

Received 24 September 2024; accepted after revision 26 December 2024; online publish-ahead-of-print 10 February 2025

Abstract

Aims

Shear wave elastography (SWE) is a new promising ultrasound modality that enables non-invasive measurement of the dynamic myocardial stiffness. The impact of varying physiological conditions on SWE measurement of left ventricular (LV) myocardial stiffness remains poorly investigated.

Methods and results

Nineteen sheep were evaluated during open-chest surgery. Epicardial multiframe SWE acquisitions were performed in short-axis view simultaneously with haemodynamic acquisitions during inferior vena cava occlusion, aortic clamping, atrial pacing, and ischaemia–reperfusion. The cyclic variation in the median value of LV myocardial stiffness ranged from 1.1 m/s in diastole (C_{\min}) to 2.4 m/s in systole (C_{\max}). At steady state, intra-animal reproducibility was good for C_{\min} [intra-class correlation coefficient ICC = 0.77 (0.54, 0.90), $P < 0.001$] and C_{\max} [ICC = 0.92 (0.84, 0.96), $P < 0.001$]. C_{\min} was independent of loading conditions, heart rate, and short 15-minute episodes of ischaemia and reperfusion. C_{\max} was independent of loading conditions and moderate increase in heart rate but decreased significantly during ischaemia and reperfusion. Compared with baseline, percentage changes in C_{\max} was correlated to percentage changes in dP/dt_{\max} ($R = 0.47$, $P = 0.001$) and in LV systolic pressure ($R = 0.35$, $P = 0.013$) and SW ($R = 0.31$, $P = 0.026$).

Conclusion

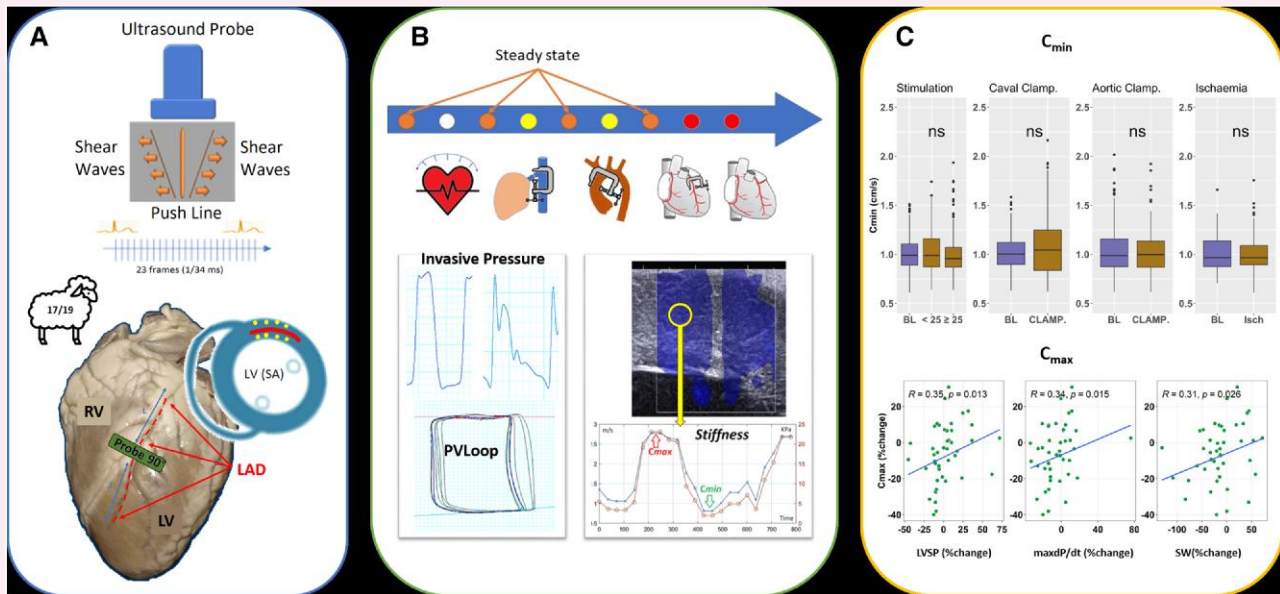
In this study, LV diastolic myocardial stiffness C_{\min} assessed using SWE demonstrated the characteristics of a potentially useful clinical marker of LV diastolic function linked to the intrinsic elastic properties of the myocardium, whereas C_{\max} was an indicator of LV contractility.

* Corresponding author. E-mail: saloux-e@chu-caen.fr

  The Author(s) 2025. Published by Oxford University Press on behalf of the European Society of Cardiology.

This is an Open Access article distributed under the terms of the Creative Commons Attribution-NonCommercial License (<https://creativecommons.org/licenses/by-nc/4.0/>), which permits non-commercial re-use, distribution, and reproduction in any medium, provided the original work is properly cited. For commercial re-use, please contact reprints@oup.com for reprints and translation rights for reprints. All other permissions can be obtained through our RightsLink service via the Permissions link on the article page on our site—for further information please contact journals.permissions@oup.com.

Graphical Abstract



SWE cardiac stiffness under conditions of load, heart rate, and ischaemia. (A) Experimental setup, RV, right ventricle; LV, left ventricle; LAD, left anterior descending artery; L, half of the LAD. (B) Time line of experimental protocol (top), haemodynamic invasive monitoring, PVLoop (bottom right), and shear wave elastography acquisition (bottom left). (C) Results, C_{min} , SWE diastolic values; C_{max} , SWE systolic values.

Keywords

shear wave elastography • myocardial stiffness • diastolic function • systolic function • ischaemia • reperfusion • animal model

Introduction

Ultrasound is the cornerstone in clinical management of patients with heart disease, allowing non-invasive morphological and haemodynamic assessment of the heart. Cardiac magnetic resonance imaging with late gadolinium enhancement or T1 mapping techniques demonstrated the prognostic value of tissue characterization in various cardiomyopathies.^{1–4} The quantification of cardiac deformation using strain analysis provides a link between anatomical tissue structures and their mechanical properties and has been proposed as a substitute for tissue characterization.^{5,6} Nevertheless, the result of strain analysis depends on physiological conditions including loading conditions and heart rate. Shear wave elastography (SWE), a recent ultrasound technological innovation initially introduced by Sarvazyan *et al.*⁷ allows tissue stiffness measurement, opening the way to tissue characterization. Shear wave elastography is based on the physical principle that links the velocity of ultrasonic waves transmitted perpendicular to the pushing axis of an acoustic force (C_T) to the shear modulus (i.e. stiffness) as expressed by the following formula, assuming a linearly elastic and isotropic tissue:

$$C_T = \sqrt{\frac{\mu}{\rho}}$$

Where C is the shear velocity, μ is the shear modulus, and ρ is the volumic mass of the tissue. This modality has demonstrated its full potential in the assessment of static superficial organs for the detection of tumours, liver fibrosis, or traumatic muscle injury.^{8–11} In cardiac imaging, it offers the potential to measure cardiac stiffness throughout the cardiac cycle, allowing the assessment of both passive stiffness

and contractile function.¹² However, in addition to the technical complexity of image acquisition, the influence of factors which potentially modulate myocardial stiffness are poorly documented, including tissue anisotropy, loading conditions, heart rate, and myocardial ischaemia or fibrosis.

The aim of the present study was to analyse the impact of changes in cardiac physiologic conditions on the measurement of left ventricular (LV) stiffness using ECG-gated SWE.

Materials and methods

Experimental protocol

Seventeen sheep (50 ± 8 kg) were evaluated. All animals received humane care in compliance with the European Convention on Animal Care. All animal procedures were performed according to the European directive 2010/63/EU on protecting animals used for scientific purposes and specific French laws (decree no. 2013–118) and were approved by the regional animal ethics committee (Comité d'Éthique Normand en Matière d'Expérimentation Animale, CENOMEXA 054) and authorized by the Ministère de l'Enseignement Supérieur, de la Recherche et de l'Innovation (APAFIS#10533-2017070617597464 v3).

Anaesthesia was induced by intramuscular injection of ketamine (3 mg/kg) and midazolam (0.1 mg/kg) and maintained by an intravenous infusion propofol (1 mL/kg/h to 2 mL/kg/h), associated with fentanyl (3 μ g/kg/h) for analgesia. The animal was intubated and placed on mechanical ventilation. The animal was then placed in a decubitus position and a sternotomy was performed. The pericardium was incised and sutured to the chest wall to form a cradle access for the heart. Invasive

monitoring of aortic pressure was performed using an 8-Fr fluid-filled pigtail catheter inserted into the femoral artery and advanced to the thoracic descending aorta. A pacing electrode was inserted through the jugular vein into the right atrium and connected to an external generator (Medtronic, Minneapolis, MN, USA). Heart rate, aortic pressure, pulse oximetry, and a 3-lead ECG were monitored throughout the experiment. Arterial blood samples with blood gas measurements were taken to adjust the ventilator parameters to pCO₂ and blood pH when necessary. From the seventh sheep onwards, LV pressure-volume curves were also recorded using a Millar 5F catheter (Millar Instrument®) connected to a Mikro-Tip® Pressure Volume System (MPVS, Millar Instrument, Houston, TX, USA) and a Quadbridge Amp amplification system (AD instruments, Oxford, UK) connected to LabChart workstation (version 8.1.16). In each animal, ECG-gated elastography acquisition sequences were performed via the epicardium using a linear probe equipped with an elastography module (Graphical Abstract). At the end of the experiment, the animals were euthanized using an overdose of anaesthetic.

The following procedures were performed as follows: (i) baseline, (ii) low (<25 bpm) and high (≥25 bpm) increase in heart rate by right atrial pacing, (iii) transient clamping of the inferior vena cava, (iv) increase in afterload by partial clamping of the ascending aorta; and (v) ischaemia/reperfusion by means of a 15-min ligation of the medial portion of the left anterior descending coronary artery followed by reperfusion. In addition, a 15–20 min recovery phase between changes in physiological conditions allowed repeated measurements of myocardial stiffness at equilibrium state. The experimental protocol is summarized in Figure 1.

Shear wave elastography

Shear wave elastography acquisitions were performed using an Aixplorer® (Supersonic® Imagine, Aix-en-Provence, France) coupled with a linear transducer SL15-4 (8 MHz, Vermon, France). As previously described,¹² cardiac SWE sequences were characterized by an accelerated repetition rate of the acoustical firing (by a factor 23) during a fixed duration (1 s). This acceleration allows to sample the measurement of myocardium elasticity adequately to capture its dynamic evolution within the cardiac cycle. An external triggering system (Lionheart, Fluke biomedical, Everett, WA, USA) was used to synchronize the acquisition to the R-wave. A B-mode image was acquired to focus the push delivery and the area of shear wave velocity measurements before switching to SWE. As previously proposed,¹³ cardiac SWE acquisitions were obtained in short axis to overcome any anisotropic effect, the short axis being obtained with the probe perpendicular to the left anterior descending coronary artery used as a landmark to insure the reproducibility of slice orientation. Acquisition sequence quality was checked immediately from the machine interface by playing the transverse shear wave sequence. Shear wave elastography acquisition sequences (11 ± 4) were performed at each phase of the protocol, and each one was time-stamped in the physiological data recording system.

Data post-processing

At the end of each experiment, data were exported and analysed offline using MATLAB® software (MATLAB R2020, MathWorks Inc., Natick, MA, USA). From RF signal, a two-dimensional map of myocardial stiffness was established, enabling regional measurements. Eight regions of interest were positioned over the myocardium, four on either side of the central shock-wave zone. In order to standardize the post-processing procedure and reduce processing time, the process has been standardized and automated using the free software Super Macro (<https://www.supermacro.fr/>). Each region of interest stiffness measurement was stored in a csv data file for further extraction of the systolic stiffness defined as maximal value (C_{max}), the diastolic

stiffness defined as minimal value (C_{min}) and to calculate the fractional change in stiffness as

$$C\% = \frac{(C_{max} - C_{min})}{C_{min}} \times 100$$

The percentage change in C values (Pc%) compared with baseline was calculated as:

$$Pc\% = \frac{(\text{Measured value} - \text{Baseline value})}{\text{Baseline value}} \times 100$$

Left ventricular end-diastolic pressure (LVEDP) and LV systolic function parameters (dP/dt_{max}, dP/dt_{min}) were extracted at each step of the protocol, and pressure-volume loops were also recorded during transient inferior vena cava clamping.¹⁴ Effective arterial elastance (E_a, defined as LVESP/SV), stroke work (defined as the area enclosed by the pressure volume loop), and contractility index [CI = dP/dt_{max} divided by the pressure (P) at the time of dP/dt_{max}] were derived from PVLoops. Haemodynamic and electrocardiographic data synchronized to SWE acquisition sequences were averaged over a 4-s period.

Statistical analysis

The normal distribution of data was evaluated using the Shapiro–Wilk test. Continuous variables were expressed as mean ± standard deviation in case of normal distribution or median (25th–75th percentiles) otherwise. Data comparisons between different interventions were performed using one-way ANOVA or Kruskal–Wallis test according to the data distribution. P values were adjusted in case of multiples pairwise comparisons. Median absolute deviation was used to suppress outliers of SWE peaks values datasets. Myocardial stiffness over the entire cardiac cycle was normalized using the formula: (Measurement—Min Value)/(Max Value—Min Value) allowing data from all animals to be merged. Intra-animal repeatability was evaluated by the comparison of all equilibrium phases for each animal, and inter-animal variability estimated by comparing the first baseline measurement. Intra-class correlation coefficient (ICC) was used for repeatability and intra and inter animal variability. Intra-class correlation coefficient values <0.5 were indicative of poor reliability, values between 0.5 and 0.75 indicated moderate reliability, values between 0.75 and 0.9 indicated good reliability, and values greater than 0.90 indicated excellent reliability. The significance threshold was set at P < 0.05. The statistical software used in this study was RStudio [RStudio Team (2020). RStudio: Integrated Development for R. RStudio, PBC, Boston, MA, USA. URL: <http://www.rstudio.com/>].

Results

Feasibility and SWE signal distribution

The feasibility of the technique was excellent, with only 9% of all acquisitions that could not be used due ECG-gating issues. After rejection of outliers, signal heterogeneity was characterized by a coefficient of variation of 16% for C_{min} and 31% for C_{max}. As shown in Figure 2, the normalized stiffness recorded over the entire cardiac cycle demonstrated a cyclic variation. After an artefact on the first frame, we observed a maximum peak at frame 10 (C_{max}) and a minimum value at frame 20 (C_{min}), approximately 430 and 870 ms after the R wave, respectively, corresponding to the systolic and diastolic stiffness.

SWE peaks measurement

As showed in Figure 3, the C_{max} and C_{min} peaks distributions were characterized by a non-normal right skewed distribution with a

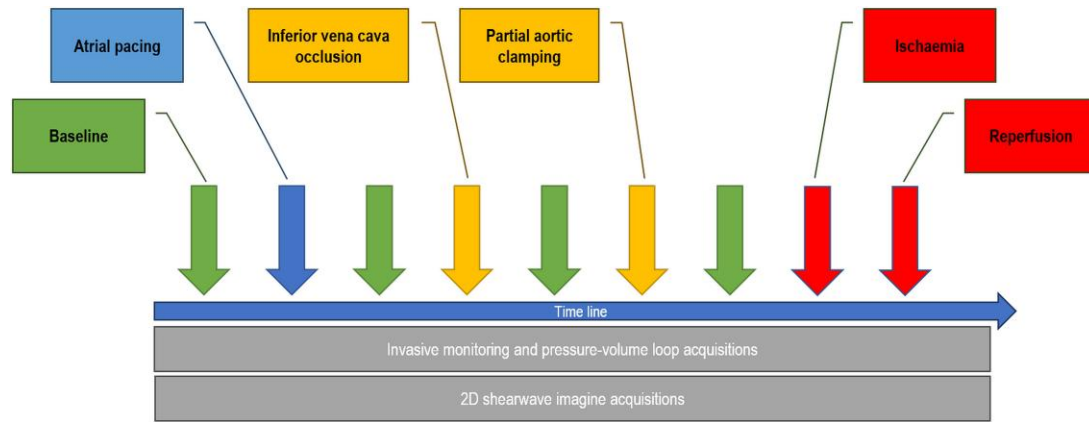


Figure 1 Timeline of the experimental protocol.

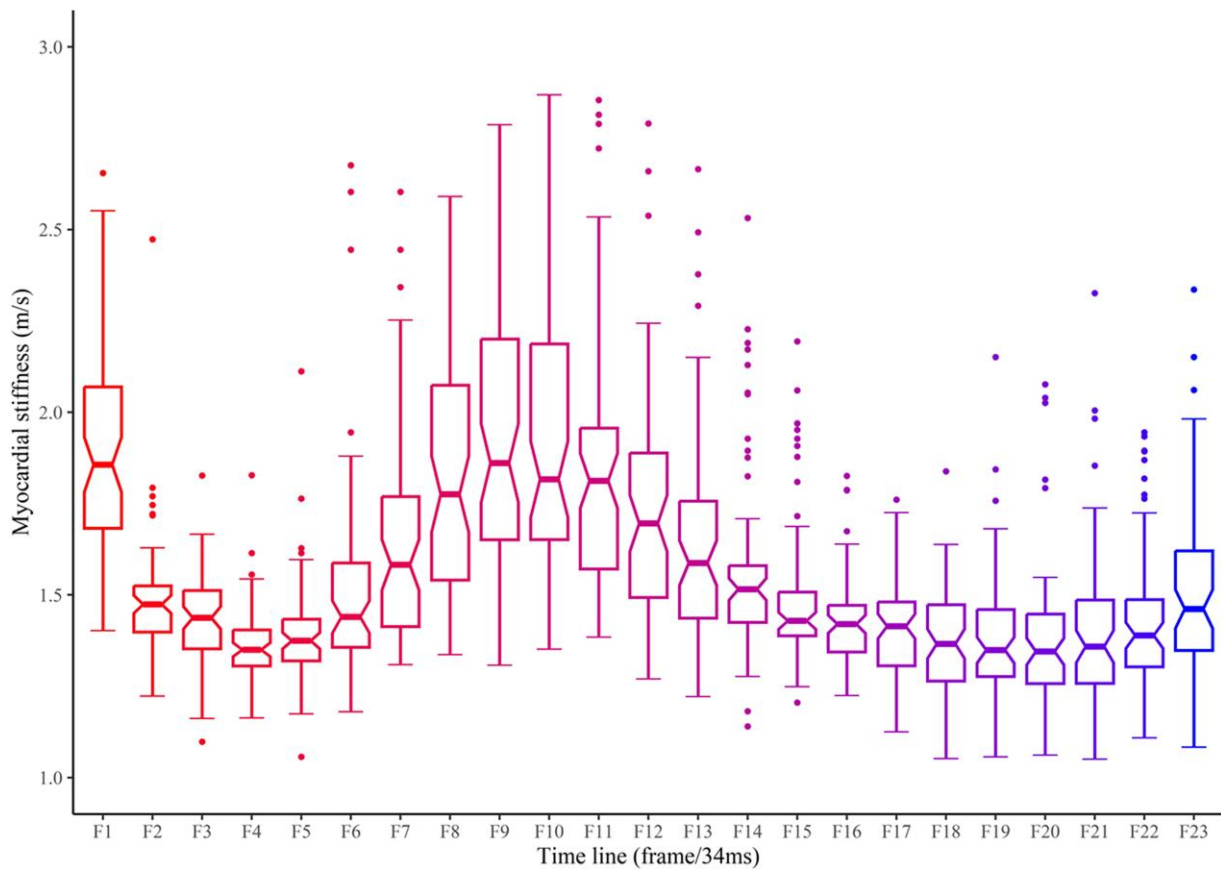


Figure 2 Cyclic variation of the cardiac stiffness values expressed in m/s: F1 to F23 represent the 23 images of the multi-shot cardiac SWE sequence.

positive skewness and kurtosis values > 3 (Figure 4). The median values obtained for C_{\max} and C_{\min} were respectively 3.12 m/s (2.33 m/s–3.80 m/s) and 0.98 m/s (0.87 m/s–1.11 m/s, $P < 0.001$), leading to a fractional change in stiffness ($C\%$) of $206\% \pm 97\%$. The repeatability of peaks measurement was high, with an ICC calculated at

0.91 (0.90, 0.93) for C_{\max} and 0.87 (0.86, 0.89) for C_{\min} (Table 1). Intra-animal reproducibility was also good when comparing all equilibrium phases for each animal (Table 1). In addition, comparison of stiffness between animals showed a statistical difference for C_{\max} but not for C_{\min} (Figure 4).

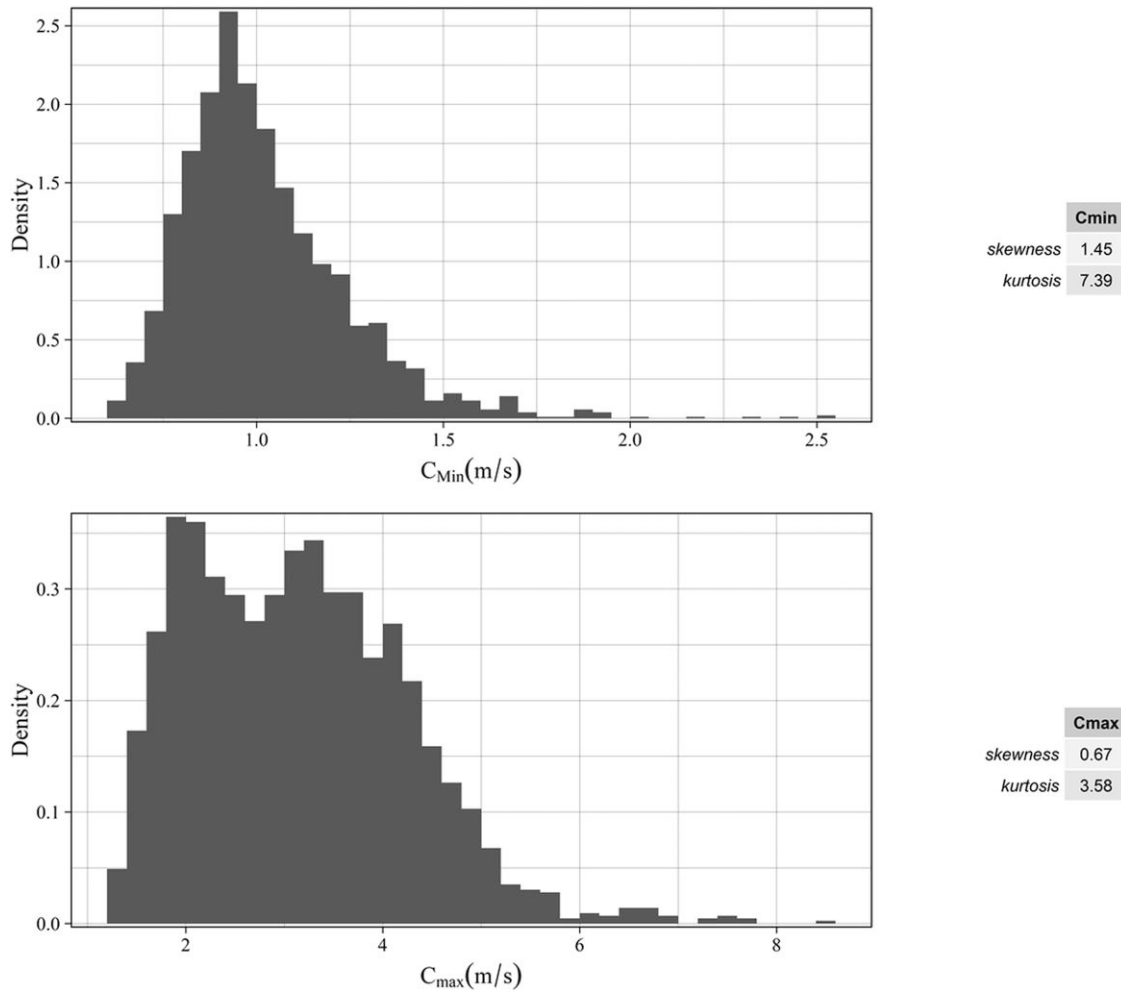


Figure 3 Distribution of C_{\min} and C_{\max} values.

Effect of heart rate and loading conditions

As showed in [Table 2](#), there was no significant effect of heart rate variation or changes in loading conditions on the results of C_{\min} despite significant haemodynamic changes during the different experimental conditions compared with baseline ([Table 3](#)). In addition, there was no significant impairment in C_{\max} during preload and afterload changes, but the percentage change in C_{\max} was significantly correlated to dP/dt_{\max} ($R = 0.47$, $P = 0.001$), LVSP ($R = 0.35$, $P = 0.013$), and SW ($R = 0.31$, $P = 0.026$; [Figure 5](#)). However, C_{\max} and $C\%$ demonstrated a biphasic behaviour during the increase in heart rate: C_{\max} and $C\%$ significantly increased with a low increase in heart rate (<25 bpm) and then decreased when the heart rate was further increased over 25 bpm. We found no significant correlation between the variations of C_{\min} and those of haemodynamic parameters ($R = -0.085$, -0.28 , -0.03 , 0.052 , 0.17 , 0.15 for systolic blood pressure, LVSP, LVEDP, heart rate, dP/dt_{\min} , Tau, respectively, all P values = ns).

Effect of ischaemia and reperfusion

Neither ischaemia nor reperfusion affected myocardial C_{\min} while there were both associated with a significant decrease in C_{\max} and $C\%$ compared with baseline (see [Table 2](#)). As shown in [Table 3](#), during ischaemia, there was a significant fall in LVSP and heart rate. In addition,

haemodynamic measurements showed a significant increase in Tau during ischaemia, followed by a decrease after reperfusion, without significant changes in dP/dt_{\max} and dP/dt_{\min} .

Correlations between SWE measurements and haemodynamic changes

No significant correlation was found between C_{\max} measurements and systolic blood pressure ($R = 0.012$, $P = \text{ns}$), systolic ventricular pressure ($R = 0.0052$, $P = \text{ns}$), heart rate ($R = 0.0035$, $P = \text{ns}$), E_a ($R = 0.08$, $P = \text{ns}$), contractility index ($R = -0.19$, $P = \text{ns}$), and stroke work ($R = 0.16$, $P = \text{ns}$). However, C_{\max} was inversely correlated to dP/dt_{\max} ($R = -0.21$, $P < 0.05$) and the variation in C_{\max} was correlated with the variation in systolic blood pressure ($R = 0.47$, $P = 0.001$), systolic ventricular pressure ($R = 0.33$, $P = 0.025$), dP/dt_{\max} ($R = 0.40$, $P = 0.006$), and contractility index ($R = 0.34$, $P = 0.019$) but not to arterial elastance E_a ($R = 0.12$, $P = \text{ns}$) ([Figure 5](#)).

Discussion

The main finding of this preclinical study is that LV diastolic stiffness measured by SWE is reproducible and independent of loading conditions, heart rate, and short episodes of ischaemia. In addition, changes

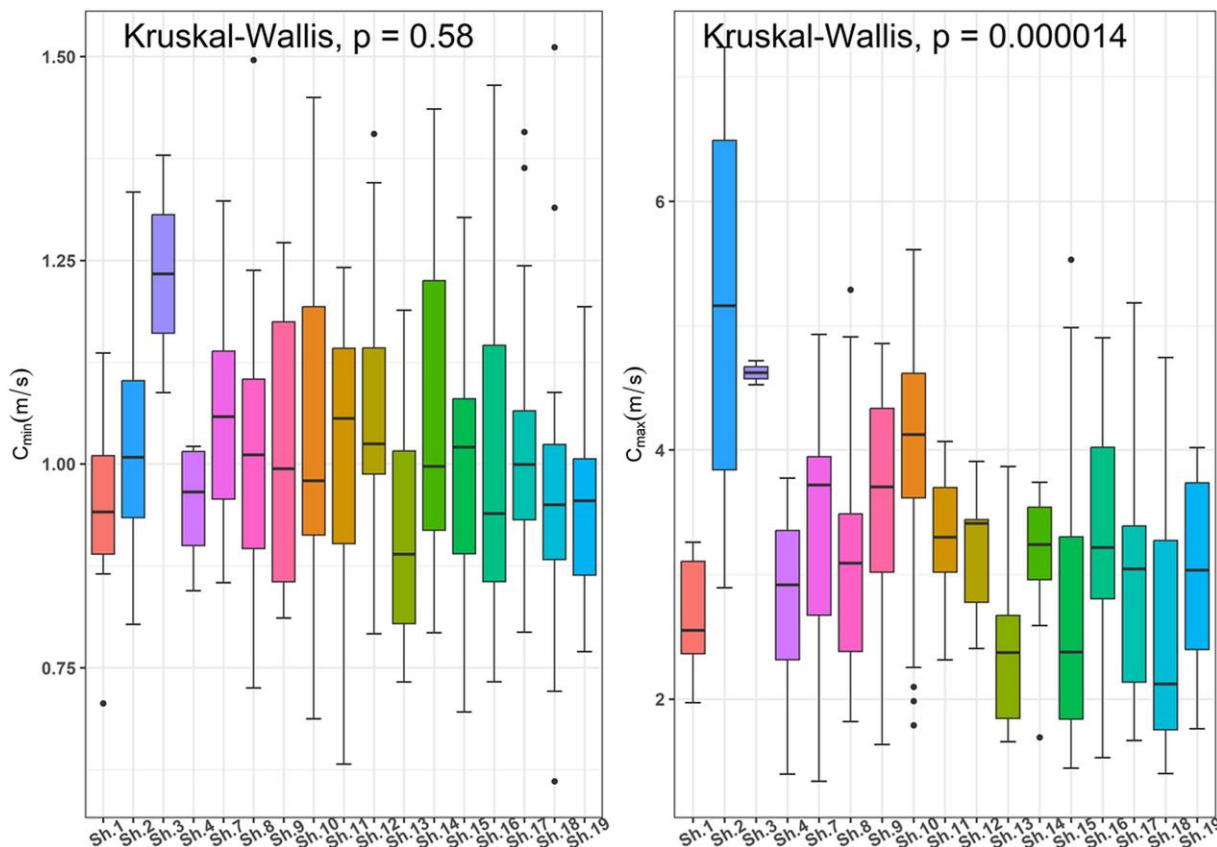


Figure 4 Inter-animal comparison of C_{\min} and C_{\max} values at first base-line phase of the experimental protocol. Sh1 to Sh.19 for Sheep 1 to 19 (data for Sheep 5 and 6 were not available: see text for details).

Table 1 Intra-class correlation coefficient for intra-individual reproducibility

Measure	ICC	P
SWE repeatability		
C_{\min}	0.87 [0.86, 0.89]	<0.001
C_{\max}	0.91 [0.90, 0.93]	<0.001
SWE intra-animal variability		
C_{\min}	0.77 [0.54, 0.90]	<0.001
C_{\max}	0.92 [0.84, 0.96]	<0.001
SWE Inter-animal variability		
C_{\min}	0.43 [0.12, 0.67]	0.01
C_{\max}	0.24 [-0.17, 0.56]	NS

SWE, shear-wave elastography; C_{\min} , diastolic left ventricular stiffness in short axis; C_{\max} , systolic left ventricular stiffness in short axis.

in systolic stiffness reflected changes in LV contractility and were impaired during ischaemia and reperfusion.

The LV passive elastic properties participate in diastolic filling and may be non-invasively accessible by measuring the propagation velocities of shear waves induced after a mechanical excitation of the tissue.^{15–17} Early results demonstrated the high agreement between

SWE-derived measurements of shear modulus and invasive end-diastolic pressure–volume relationship.¹⁸ Changes in pre- or after-load may theoretically alter the magnitude of the forces exerted on the ventricular wall and modify the level of the stress–strain relationship of the cardiac muscle.

Diastolic stiffness

Our results demonstrated the independence of LV diastolic stiffness measurements from loading conditions, heart rate, and short episodes of ischaemia, opening the way to potential clinical applications. Pernot et al.¹⁹ showed in a Langendorff perfused isolated adult rat heart that LV diastolic myocardial stiffness did not change significantly with pre-load increase. These results were consistent with early findings¹⁷ using multifrequency shear wave dispersion method *in vivo* in pigs, showing no significant change in diastolic shear elastic modulus in normal animals during pre-load increase. The load independence of diastolic stiffness measured by SWE has also been reported by Caenen et al.²⁰ using a transthoracic approach in pigs. Our results are in agreement with these previous studies. Despite significant variations in LV end-diastolic pressure during inferior vena cava occlusion and partial aortic clamping, we did not observe any significant variation in LV diastolic stiffness. The load-independence of diastolic stiffness assessed by active ARFI opens the way to the measurement of passive mechanical properties of the heart in several clinical situations, including heart failure (with preserved or reduced ejection fraction), aortic stenosis, or hypertrophic cardiomyopathy.

Table 2 Myocardial stiffness according to phase provocation

Atrial stimulation	Baseline	Δ FRC < 25 bat/mn	Δ FRC \geq 25 bat/mn	P
N ROIs	259	234	266	
C_{\min} (m/s) [median (IQR)]	0.99 [0.89, 1.10]	0.96 [0.87, 1.08]	0.94 [0.86, 1.05]	0.126
C_{\max} (m/s) [median (IQR)]	3.19 [2.27, 3.92]	3.44 [2.86, 4.13]	2.49 [2.08, 3.21]**	<0.001
C% [median (IQR)]	211 [152, 282]	239 [184, 305]	162 [130, 222]**	<0.001

Vena cava clamping	Baseline	Clamping	P
C_{\min} (m/s) [median (IQR)]	1.00 [0.90, 1.12]	1.03 [0.82, 1.23]	0.362
C_{\max} (m/s) [median (IQR)]	3.22 [2.54, 3.91]	3.18 [2.30, 4.08]	0.814
C% [median (IQR)]	211 [158, 276]	198 [113, 258]	0.057

Partial aortic clamping	Baseline	Clamping	P
C_{\min} (m/s) [median (IQR)]	0.98 [0.87, 1.12]	1.00 [0.87, 1.14]	0.684
C_{\max} (m/s) [median (IQR)]	3.16 [2.25, 3.79]	3.02 [2.17, 4.04]	0.636
C% [median (IQR)]	188 [141, 244]	192 [124, 272]	0.896

Ischaemia/reperfusion	Baseline	Ischaemia	Reperfusion	P
C_{\min} (m/s) [median (IQR)]	0.95 [0.86, 1.11]	0.96 [0.89, 1.09]	0.93 [0.83, 1.05]	0.090
C_{\max} (m/s) [median (IQR)]	3.07 [2.45, 3.63]	2.75 [2.11, 3.54]*	2.32 [1.90, 3.07]**	<0.001
C% [median (IQR)]	189 [151, 248]	172 [123, 249]*	156 [103, 213]**	<0.001

C_{\min} , minimal shearwave transverse velocity; C_{\max} , maximal shearwave transverse; C%, shearwave transverse velocity percentage of variation. * $P < 0.05$ for comparisons with baseline. ** $P < 0.05$ between large and small increase in heart rate. *** $P < 0.05$ between ischaemia and reperfusion.

Systolic stiffness

Left ventricular systolic stiffness is a marker of contractility, as suggested by its increase during cardiac contraction,^{19,21,22} its dependence on myocardial perfusion,²² the cellular concentrations of Ca^{2+} , and the effect of isoproterenol.¹⁹ However, these physiologically relevant findings demonstrated in isolated hearts do not predict the indirect and more clinically relevant effect of a moderate increase in afterload. In our study, partial aortic clamping induced a reasonable increase of approximately 20 mmHg in LV systolic pressure, which corresponds to physiological variations in human blood pressure. Under these conditions, variations in systolic stiffness were correlated with variations of LV systolic pressure and LV contractility as shown by dP/dt_{\max} and contractility index, but not with the arterial elastance, which reflects afterload. In addition to previous findings,^{20,23} our study further demonstrated that during partial aortic clamping, which induced a mild but significant increase in LV contractility, individual variations in systolic stiffness were correlated with the variation of left ventricular contractility compared with baseline.

Impact of heart rate

Regarding the possible impact of heart rate, our results demonstrated no significant changes in diastolic stiffness during atrial pacing within a physiologic range of heart rate increase, which is consistent with the significant decrease in LVEDP for the highest heart rate values. Previous findings from Pernot *et al.*¹⁹ emphasized that a significant increase in LV diastolic stiffness may occur only with an extreme increase in heart rate, most likely due to incomplete myocardial relaxation.²⁴ In addition, our results demonstrated a reduction in LV systolic stiffness at higher

heart rate. The inotropic effect induced by pacing was negligible, as indicated by the absence of changes in the maximum rate of LV pressure rise (dP/dt_{\max}), whereas under spontaneous activity the heart rate increase is associated with an increase in dP/dt_{\max} as a consequence of increasing sympathetic tone and contractility.²⁵ However, as the temporal sampling of the SWE signal remains unchanged throughout the experiment (set at 23 frames per second), it is very likely that the apparent decrease in systolic stiffness at high heart rate is related to an under-sampling of SWE at a high heart rate.

Ischaemia and reperfusion

Reperfusion following acute myocardial infarction results in myocardial interstitial oedema, which is responsible for an increase in wall thickness and stiffness.²⁶ Preclinical experiments from Pislaru *et al.*¹⁷ demonstrated an increase in both diastolic and systolic stiffness in pigs submitted to a 1–3 h occlusion of the left anterior descending coronary artery followed by 1–2 h of reperfusion. Pernot *et al.*¹³ compared the results of shear wave imaging in animals after a coronary artery ligation for 15 min (stunning group) or 2 h (infarction group) followed by a 40-min reperfusion. In this study, only prolonged ischaemia (>120 min) resulted in a significant increase in diastolic stiffness from 1.7 ± 0.4 to 6.2 ± 2.2 kPa ($P < 0.05$), further increased after reperfusion to 12.1 ± 4.2 kPa; $P < 0.01$, while it remained unchanged in the stunned group (2.3 ± 0.4 kPa vs. 1.8 ± 0.3 kPa, $P = ns$). These results were recently confirmed using natural SWE as an alternative method for the assessment of myocardial stiffness after a 90-min coronary artery occlusion.²³ In the present study, we emphasize that a short 15-min coronary artery occlusion, mimicking a clinically relevant

Table 3 Haemodynamic changes during experimental phases

Atrial stimulation	Baseline	Δ HR < 25 bat/mn	Δ HR ≥ 25 bat/mn	P
HR [bat.:mn; mean (SD)]	88.96 (19.81)	111.55 (16.37)	115.92 (10.39)*	<0.001
SBP [mmhg; mean (SD)]	68.20 (17.53)	64.45 (13.26)	78.22 (23.28)*	<0.001
DBP [mmhg; mean (SD)]	48.97 (15.03)	45.92 (8.85)	56.67 (20.04)*	<0.001
LVSP [mmhg; mean (SD)]	71.18 (16.71)	65.77 (17.29)	68.10 (29.86)	0.027
LVEDP [mmhg; mean (SD)]	17.48 (3.82)	19.66 (3.68)	14.27 (4.00)	0.049
dP/dt _{max} (mmHg/s)	745.72 (132.62)	693.84 (215.13)	789.39 (118.68)	0.333
dP/dt _{min} (mmHg/s)	-482.35 (124.66)	-427.55 (102.10)	-576.47 (148.65)	0.030
Tau (ms)	113 (35)	117 (17)	91 (23)	0.050
Contractility index [1/s; mean (SD)]	19.35 (3.28)	17.56 (3.62)	22.79 (5.33)	0.069
SW [mean (SD)]	794.00 (403.09)	523.51 (521.18)	327.74 (292.32)	0.216
Ea [mean (SD)]	4.80 (1.71)	4.95 (2.25)	7.20 (2.10)	0.111

Inferior vena cava clamping	Baseline	Clamping	P
HR [bat.:mn; mean (SD)]	89.31 (22.27)	94.57 (18.54)	0.028
SBP [mmhg; mean (SD)]	68.01 (19.13)	62.57 (13.84)	0.006
DBP [mmhg; mean (SD)]	47.25 (17.58)	39.96 (11.20)	<0.001
LVSP [mmhg; mean (SD)]	68.50 (22.29)	57.52 (24.57)	<0.001
LVEDP [mmhg; mean (SD)]	14.74 (1.83)	13.05 (2.18)	0.017
dP/dt _{max} (mmHg/s)	722.68 (127.29)	568.76 (150.27)	0.002
dP/dt _{min} (mmHg/s)	-475.61 (128.37)	-342.02 (120.28)	0.002
Tau (ms)	77 (35)	150 (60)	<0.001
Contractility index [1/s; mean (SD)]	19.22 (4.22)	17.98 (4.61)	0.524
SW [mean (SD)]	821.36 (389.04)	781.42 (318.86)	0.778
Ea [mean (SD)]	4.45 (1.55)	4.14 (2.47)	0.752

Partial aortic clamping	Baseline	Clamping	P
HR [bat.:mn; mean (SD)]	92.11 (14.72)	91.45 (20.60)	0.775
SBP [mmhg; mean (SD)]	72.68 (11.91)	75.62 (12.60)	0.061
DBP [mmhg; mean (SD)]	50.45 (10.48)	47.44 (12.38)	0.040
LVSP [mmhg; mean (SD)]	63.38 (23.79)	83.64 (34.86)	<0.001
LVEDP [mmhg; mean (SD)]	14.74 (1.83)	16.91 (2.39)	0.004
dP/dt _{max} (mmHg/s)	722.68 (127.29)	798.06 (139.10)	0.090
dP/dt _{min} (mmHg/s)	-475.61 (128.37)	-608.10 (125.40)	0.002
Tau (ms)	77 (35)	71 (12)	0.313
Contractility index [1/s; mean (SD)]	20.01 (5.04)	18.55 (4.20)	0.431
SW [mean (SD)]	715.31 (988.39)	743.72 (1605.78)	0.965
Ea [mean (SD)]	3.69 (1.81)	3.94 (2.42)	0.795

Ischaemia/reperfusion	Baseline	Ischaemia	Reperfusion	P
HR [bat.:mn; mean (SD)]	89.88 (19.54)	81.94 (21.94)	87.52 (19.14)	0.002
SBP [mmhg; mean (SD)]	64.01 (18.08)	61.84 (29.10)	59.90 (8.20)	0.100
DBP [mmhg; mean (SD)]	45.82 (19.27)	40.01 (12.42)	41.77 (9.53)	0.001
LVSP [mmhg; mean (SD)]	65.36 (18.01)	60.88 (13.42)	57.39 (15.32)	<0.001
LVEDP [mmhg; mean (SD)]	14.78 (1.34)	15.64 (0.77)	14.99 (0.23)	0.569
dP/dt _{max} (mmHg/s)	758.55 (132.44)	630.56 (121.12)	522.72 (172.89)	0.007
dP/dt _{min} (mmHg/s)	-468.47 (89.24)	-411.26 (98.11)	-352.01 (74.04)	0.024
Tau [mean (SD)]	80.37 (33.51)	102.15 (20.77)	114.70 (19.51)	0.015

Continued

Table 3 Continued

Ischaemia/reperfusion	Baseline	Ischaemia	Reperfusion	P
Contractility index [1/s; (mean (SD))]	-158.86 (468.16)	16.52 (1.86)	13.99 (3.74)	0.17
SW [mean (SD)]	479.22 (1060.72)	841.90 (444.05)	584.36 (762.21)	0.535
Ea [mean (SD)]	4.15 (2.91)	5.96 (7.29)	2.82 (1.03)	0.268

HR, heart rate; SBP, systolic blood pressure; DBP, diastolic blood pressure; LVSP, left ventricular systolic pressure; LVEDP, left ventricular end diastolic pressure; bpm, beat per minute; SD, standard deviation. * $P < 0.05$ vs. baseline.

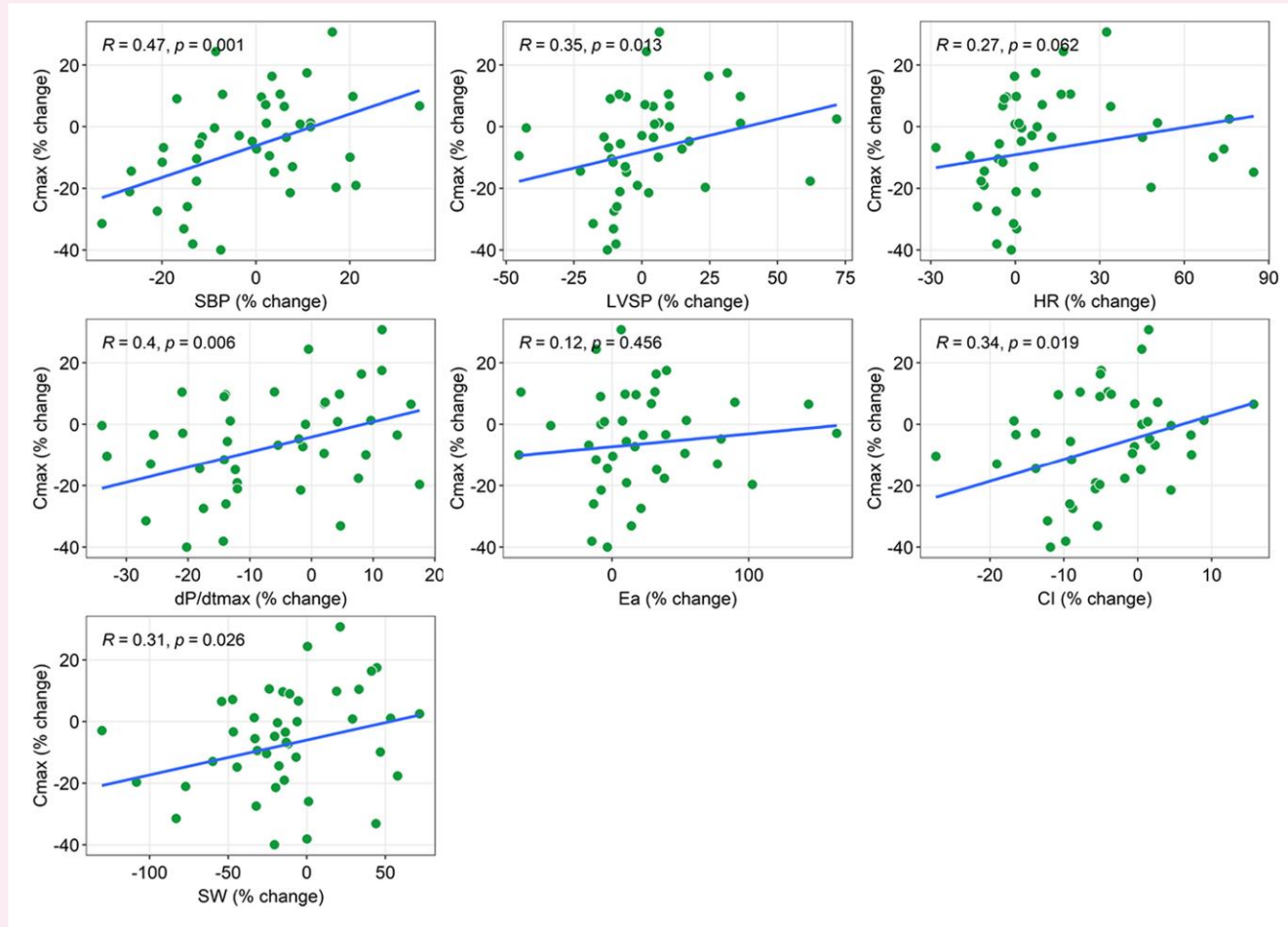


Figure 5 Correlations between variation of systolic stiffness and haemodynamic parameters. SBP, systolic blood pressure; LVSP, left ventricular systolic pressure; HR, heart rate; dP/dt max, maximal rate of rise of left ventricular pressure; EA, arterial elastance; CI, contractility index; SW, stroke work.

episode of ischaemia, did not modify the diastolic stiffness. However, ischaemia resulted in an impairment of systolic stiffness, which lasted after reperfusion, suggesting that myocardial stunning could be identified by the association of decreased systolic stiffness with a preserved diastolic stiffness.

Signal properties

Multi-shot SWE sequence demonstrated high feasibility. However, despite acquisitions on a short axis to reduce the effect of anisotropy,^{15,21} some recorded stiffness curves were rejected due to noise in the SWE

signal, as previously described.^{12,27} This phenomenon may be favoured by the multi-shot cardiac SWE technique¹² and the small size of the ROIs (3.6×3.6 mm).²⁸ Due to the non-normal distribution of the speeds of each animal, we applied a median absolute deviation filter adapted and not an arbitrary threshold as previously proposed.^{18,22}

Limitations of the study

A heterogeneity in animals' weight and their haemodynamic condition at the start of and throughout the experiment may have promoted a variability in the measurements. However, this situation may, to a

certain extent, be transposed to human in a more clinical approach. Similarly, the acquisitions and measurement regions were not absolutely similar in all animals, increasing the effect of anisotropy and the variability of our measurements. Electrolyte imbalances were not evaluated in the present study, although they could impact systolic contractility and diastolic relaxation. In addition, propofol may interact with contractility and diastolic relaxation, via a modulation of phosphorylation and a reduction in afterload.²⁹ Further studies on the role of SWE in detecting changes in myocardial stiffness under electrolyte imbalance and anaesthesia would be beneficial.

The multi-shot SWE sequence used in this study was triggered by the R-Peak of the ECG trace at a fixed rate of 23 frames per second. As a result, diastolic and systolic SWE measurements were not acquired at a specific time of the cardiac cycle but defined on the maximum and minimum of the SWE curve. A high heart rate may be associated with signal undersampling, which could have altered systolic measurements, especially during high rate atrial pacing. Finally, in order to avoid epicardial probe pressure and cavity artefact in the subendocardium, we chose to limit the measurement to a medial zone of the myocardium. Consequently, we were unable to characterize SW velocity as a function of transmural. Finally, direct comparison with emerging non-invasive ultrasound technique for assessing cardiac function, such as Myocardial Work, was not available in this animal model and was outside the scope of this study.

Conclusion

In this study, LV systolic stiffness was affected by afterload and ischaemia, whereas LV diastolic stiffness was unaffected by loading conditions, contractility or heart rate. These promising results strongly suggest that SWE of diastolic stiffness could be a useful tool for tissue characterization in human.

Clinical perspectives

The SWE technique for the measurement of diastolic myocardial stiffness was independent of haemodynamic parameters and short episode of ischaemia, offering a new and specific technique to assess myocardial passive mechanical properties. This technique may be especially useful in patients with heart failure with preserved ejection fraction or with various cardiomyopathies associated with hypertrophy and/or diastolic dysfunction. In addition, systolic stiffness, which was related to myocardial contractility but not to preload could be used as a useful contractility index.

Future studies in humans using a transthoracic approach with dedicated clinical ultrasound equipment are needed to confirm the contribution of these new parameters.

Acknowledgements

The authors want to thank Ludovic Dillon, Palma Pro, and Romaric Saulnier for their useful technical support.

Author contributions

All authors contributed to the study conception and design. Material preparation, anesthesia, data collection and analysis were performed by Eric Saloux, Alain Manrique and Christophe Simard. Pauline Ruello, Vladimir Saplaçan were in charge of surgical procedures. Alexandre Lebrun and Pierre-Antoine Dupont were in charge of material preparation and data acquisition. Amir Hodzic Christophe Tribouilloy and H el ene Eltchaninoff provided a critical reviewing of the manuscript. Morgane Le Garrec and Christophe Fraschini were in charge of Cardiac 2-dimensional Shear Wave Elastography implementation. Conception, study design and first draft of the manuscript was

driven by Eric Saloux and Alain Manrique. All authors commented on previous versions of the manuscript. All authors read and approved the final manuscript.

Ethics approval

All experimental procedures and protocols used in this investigation were reviewed and approved by the Ethical Committee for animal experimentation of the Normandy Region (CENOMEXA) and authorized by the Minist ere de l'Enseignement Sup erieur, de la Recherche et de l'Innovation (APAFIS#10533-2017070617597464 v6).

Generative AI

No AI generative tools were used in this work.

Consent

Not relevant: animal study.

Funding

Research funded by Agence Nationale de la Recherche (ANR) under the program 'Investissements d'avenir' with the reference ANR-16-RHUS-0003, and was conducted as part of the FHU CARNAVAL project (GSC G4).

Conflict of interest: E.S., C.S., P.R., A.M., A. Lemaitre, A.H., A. Lebrun, P.-A.D., V.S., H.E., and C.T. declare they have no financial interests directly or indirectly related to the work submitted for publication. M.L.G. and C.F. are employees of SuperSonic Imagine.SA.

Data availability

Our raw and post-processed data can be shared on reasonable request to the corresponding author.

Lead author biography



Eric Saloux is a senior cardiologist in charge of the echocardiography laboratory at the Centre Hospitalier Universitaire de Caen Normandie. His research work focuses on technological innovations in ultrasound and their application to clinical practice. He is also involved in echocardiography training programs dedicated to young cardiologists.

References

1. Gulati A, Jabbour A, Ismail TF, Guha K, Khwaja J, Raza S et al. Association of fibrosis with mortality and sudden cardiac death in patients with nonischemic dilated cardiomyopathy. *JAMA* 2013;**309**:896–908.
2. Roes SD, Kelle S, Kaandorp TAM, Kokocinski T, Poldermans D, Lamb HJ et al. Comparison of myocardial infarct size assessed with contrast-enhanced magnetic resonance imaging and left ventricular function and volumes to predict mortality in patients with healed myocardial infarction. *Am J Cardiol* 2007;**100**:930–6.
3. O'Hanlon R, Grasso A, Roughton M, Moon JC, Clark S, Wage R et al. Prognostic significance of myocardial fibrosis in hypertrophic cardiomyopathy. *J Am Coll Cardiol* 2010;**56**:867–74.

4. Musa TA, Treibel TA, Vassiliou VS, Captur G, Singh A, Chin C et al. Myocardial scar and mortality in severe aortic stenosis. *Circulation* 2018;**138**:1935–47.
5. Cikes M, Sutherland GR, Anderson LJ, Bijnsen BH. The role of echocardiographic deformation imaging in hypertrophic myopathies. *Nat Rev Cardiol* 2010;**7**:384–96.
6. Gao L, Zhang L, Zhang Z, Lin Y, Ji M, He Q et al. Clinical utility of strain imaging in assessment of myocardial fibrosis. *J Clin Med* 2023;**12**:743.
7. Sarvazyan AP, Rudenko OV, Swanson SD, Fowlkes JB, Emelianov SY. Shear wave elasticity imaging: a new ultrasonic technology of medical diagnostics. *Ultrasound Med Biol* 1998;**24**:1419–35.
8. Luo C, Lu L, Zhang W, Li X, Zhou P, Ran Z. The value of shear wave elastography in the diagnosis of breast cancer axillary lymph node metastasis and its correlation with molecular classification of breast masses. *Front Oncol* 2022;**12**:846568.
9. Hazem M, Zakaria OM, Daoud MYI, Al Jabr IK, AlYahya AA, Hassanein AG et al. Accuracy of shear wave elastography in characterization of thyroid nodules in children and adolescents. *Insights Imaging* 2021;**12**:128.
10. Li G, Li D-W, Fang Y-X, Song YJ, Deng ZJ, Gao J et al. Performance of shear wave elastography for differentiation of benign and malignant solid breast masses. *PLoS One* 2013;**8**:e76322.
11. Zhou X, Wang C, Qiu S, Mao L, Chen F, Chen S. Non-invasive assessment of changes in muscle injury by ultrasound shear wave elastography: an experimental study in contusion model. *Ultrasound Med Biol* 2018;**44**:2759–67.
12. Saloux E, Garrec ML, Menet N, Dillon L, Simard C, Frascini C et al. Cardiac 2-D shear wave imaging using a new dedicated clinical ultrasound system: a phantom study. *Ultrasound Med Biol* 2024;**50**:843–51.
13. Pernot M, Lee W-N, Bel A, Mateo P, Couade M, Tanter M et al. Shear wave imaging of passive diastolic myocardial stiffness. *JACC Cardiovasc Imaging* 2016;**9**:1023–30.
14. Burkhoff D, Mirsky I, Suga H. Assessment of systolic and diastolic ventricular properties via pressure-volume analysis: a guide for clinical, translational, and basic researchers. *Am J Physiol Heart Circ Physiol* 2005;**289**:H501–12.
15. Pernot M, Lee W-N, Bel A, Mateo P, Couade M, Tanter M et al. Shear wave imaging of passive diastolic myocardial stiffness: stunned versus infarcted myocardium. *Jacc Cardiovasc Imaging* 2016;**9**:1023–30.
16. Vejdani-Jahromi M, Freedman J, Kim Y-J, Trahey GE, Wolf PD. Assessment of diastolic function using ultrasound elastography. *Ultrasound Med Biol* 2018;**44**:551–61.
17. Pislaru C, Urban MW, Pislaru SV, Kinnick RR, Greenleaf JF. Viscoelastic properties of normal and infarcted myocardium measured by a multifrequency shear wave method: comparison with pressure-segment length method. *Ultrasound Med Biol* 2014;**40**:1785–95.
18. Vejdani-Jahromi M, Freedman J, Trahey GE, Wolf PD. Measuring intraventricular pressure using ultrasound elastography. *J Ultrasound Med* 2019;**38**:1167–77.
19. Pernot M, Couade M, Mateo P, Crozatier B, Fischmeister R, Tanter M. Real-Time assessment of myocardial contractility using shear wave imaging. *J Am Coll Cardiol* 2011;**58**:65–72.
20. Caenen A, Keijzer L, Bézy S, Duchenne J, Orłowska M, Van Der Steen AFW et al. Continuous shear wave measurements for dynamic cardiac stiffness evaluation in pigs. *Sci Rep* 2023;**13**:17660.
21. Couade M, Pernot M, Messas E, Thomas JL, Fink M. In vivo quantitative mapping of myocardial stiffening and transmural anisotropy during the cardiac cycle. *IEEE Trans Med Imaging* 2011;**30**:295–305.
22. Vejdani-Jahromi M, Freedman J, Nagle M, Kim Y-J, Trahey GE, Wolf PD. Quantifying myocardial contractility changes using ultrasound-based shear wave elastography. *J Am Soc Echocardiogr* 2017;**30**:90–6.
23. Bézy S, Duchenne J, Orłowska M, Caenen A, Amoni M, Ingelaere S et al. Impact of loading and myocardial mechanical properties on natural shear waves. *JACC Cardiovasc Imaging* 2022;**15**:2023–34.
24. Weisfeldt ML, Frederiksen JW, Yin FCP, Weiss JL. Evidence of incomplete left ventricular relaxation in the dog. *J Clin Invest* 1978;**62**:1296–302.
25. Markert M, Trautmann T, Groß M, Ege A, Mayer K, Guth B. Evaluation of a method to correct the contractility index LVdP/dtmax for changes in heart rate. *J Pharmacol Toxicol Methods* 2012;**66**:98–105.
26. Garcia-Dorado D, Andres-Villarreal M, Ruiz-Meana M, Inserte J, Barba I. Myocardial edema: a translational view. *J Mol Cell Cardiol* 2012;**52**:931–9.
27. O'Hara S, Zelesco M, Rocke K, Stevenson G, Sun Z. Reliability indicators for 2-dimensional shear wave elastography. *J Ultrasound Med* 2019;**38**:3065–71.
28. Nitta N, Yamakawa M, Hachiya H, Shiina T. A review of physical and engineering factors potentially affecting shear wave elastography. *J Med Ultrason* 2021;**48**:403–14.
29. Ammar A, Mahmoud K, Elkersh A, Kasemy Z. A randomised controlled trial comparing the effects of propofol with isoflurane in patients with diastolic dysfunction undergoing coronary artery bypass graft surgery. *Anaesthesia* 2016;**71**:1308–16.